

## Nanoscale Devices | Very Important Paper |

VIP

Photoactive Molecular-Based Devices, Machines and Materials:  
Recent AdvancesMassimo Baroncini,<sup>[a,b]</sup> Martina Canton,<sup>[a,c]</sup> Lorenzo Casimiro,<sup>[a,c]</sup> Stefano Corra,<sup>[a,b]</sup>  
Jessica Groppi,<sup>[a,b]</sup> Marcello La Rosa,<sup>[a,b]</sup> Serena Silvi,<sup>[a,c]</sup> and Alberto Credi<sup>\*[a,b]</sup>

**Abstract:** Molecular and supramolecular-based systems and materials that can perform predetermined functions in response to light stimulation have been extensively studied in the past three decades. Their investigation continues to be a highly stimulating topic of chemical research, not only because of the inherent scientific value related to a bottom-up approach to functional nanostructures, but also for the prospective applications in diverse fields of technology and medicine. Light is an important tool in this context, as it can be conveniently used

both for supplying energy to the system and for probing its states and transformations. In this microreview we recall some basic aspects of light-induced processes in (supra)molecular assemblies, and discuss their exploitation to implement novel functionalities with nanostructured devices, machines and materials. To this aim we illustrate a few examples from our own recent work, which are meant to illustrate the trends of current research in the field.

## 1. Introduction

The interaction between light and matter is at the basis of life on our planet.<sup>[1]</sup> Photosynthesis converts large amounts of sunlight energy to power the natural world, while the information content of photons is exploited in vision-related processes. A variety of functions can also be obtained when light interacts with artificial systems; research in the past decades has shown that the nature and utility of such functions are largely determined by the chemical complexity and organization of the matter that receives and processes the photons.<sup>[2–4]</sup>

In this regard, with the development of supramolecular chemistry, it was proposed that the concept of macroscopic device and machine could be applied to the molecular level.<sup>[5–7]</sup> Briefly, a molecular device can be defined<sup>[8]</sup> as an assembly of a discrete number of molecular components designed to perform a function under appropriate external stimulation. Particularly interesting types of molecular devices are molecular

machines and motors,<sup>[8–11]</sup> whose operation involves controlled mechanical movements of their components against random thermal (Brownian) motion, activated by an energy supply.<sup>[12]</sup> The high scientific value of these ideas and their huge – and, at present, largely unexpressed,<sup>[13,14]</sup> – potential for applications led to the award of the Nobel Prize in Chemistry in 2016 to Sauvage, Stoddart and Feringa “for the design and synthesis of molecular machines”.<sup>[15–17]</sup>

Biomolecular devices and machines carry out crucial tasks in living organisms. They constitute compelling examples of the feasibility and utility of nanotechnology,<sup>[18]</sup> and provide a solid motivation for attempting the realization of artificial versions. The bottom-up synthesis of systems as sophisticated as those present in Nature is, however, a prohibitive task. Therefore, chemists have focused on the construction of much simpler species (that do not attempt to mimic the complexity of biological structures), on the investigation and rationalization of the phenomena at the basis of their operation, and on the study of their connection with the macroscopic world, particularly with regard to energy supply and information exchange.<sup>[19]</sup> In the past two decades the application of a device-driven approach to chemical research, enabled by the continuous progress in synthetic and characterization techniques and methodologies, has led to remarkable accomplishments.<sup>[20–24]</sup>

Molecular devices and machines, like their macroscopic counterparts, need an energy supply and a control system. Light provides an answer to this dual requirement: on the one hand, photons can trigger reactions that bring about structural and/or electronic modifications, which are reflected in the change of properties. Light can also be used to control and monitor the operation of the device, because the interactions between the components often affect the photonic response of the system.

[a] CLAN-Center for Light Activated Nanostructures,  
Istituto per la Sintesi Organica e la Fotoreattività, Consiglio Nazionale  
delle Ricerche, Via Gobetti 101, 40129 Bologna, Italy  
E-mail: alberto.credi@isof.cnr.it  
Web: www.credi-group.it

[b] Dipartimento di Scienze e Tecnologie Agro-alimentari,  
Università di Bologna,  
Viale Fanin 50, 40127 Bologna, Italy

[c] Dipartimento di Chimica “G. Ciamician”,  
Università di Bologna,  
Via Selmi 2, 40126 Bologna, Italy

ORCID(s) from the author(s) for this article is/are available on the WWW  
under <https://doi.org/10.1002/ejic.201800923>.

© 2018 The Authors. Published by Wiley-VCH Verlag GmbH & Co. KGaA. •  
This is an open access article under the terms of the Creative Commons  
Attribution-NonCommercial-NoDerivs License, which permits use and distribution  
in any medium, provided the original work is properly cited, the use  
is non-commercial and no modifications or adaptations are made.

It should be recalled that a key paradigm for the development of molecular-scale devices and machines is molecular switching. This phenomenon – which involves the reversible transformation of a molecular species, induced by an external stimulus, between (at least) two forms with different properties – has been widely investigated in solution and can also take



**Massimo Baroncini** received his MSc (2006) and PhD (2010) in Chemical Sciences from the University of Bologna. His PhD dissertation was awarded with the Springer Thesis Prize 2010. He is currently a postdoctoral researcher in the group of Prof. Alberto Credi. The research activity of Dr. Baroncini deals with the synthesis and investigation of supramolecular systems with tailored physico-chemical functionalities.



**Martina Canton** received her MSc in Chemical Sciences from the University of Ferrara in 2017, where she worked on nanostructured semiconductor photoanodes for photovoltaics and water splitting. In November 2017 she started her PhD in Chemistry at the University of Bologna under the supervision of Prof. Alberto Credi. Her current research activity is focused on the spectroscopic and photochemical investigation of molecular switches and motors.



**Lorenzo Casimiro** received his MSc cum laude in Photochemistry and Molecular Materials from the University of Bologna in 2016. He is currently a PhD student in the Center for Light Activated Nanostructures (CLAN) in Bologna, under the supervision of Prof. Serena Silvi. His research activity is focused on photochemistry and supramolecular chemistry, particularly on the photoinduced motion of molecular machines and motors.



**Stefano Corrà** graduated in Industrial Chemistry in 2012 at the University of Padova. He then pursued his doctoral studies in the group of Prof. Helma Wennemers (ETH Zürich) on the use of peptides for controlling the formation of supramolecular nanostructures. In 2017 he joined the Credi group as a postdoctoral fellow to work on the synthesis of dynamic supramolecular structures and the study of out-of-equilibrium synthetic systems.



**Jessica Groppi** received her MSc in Chemistry in 2010 from the University of Parma. In 2016 she completed her PhD at Queen Mary University of London (UK), working on the controlled modification of electrode surfaces through solid phase synthesis, for the development of glucose biosensors. In 2016 she joined the Credi group as a postdoctoral fellow, where she is currently involved in the synthesis and characterization of supramolecular systems and materials.



**Marcello La Rosa** received his MSc in Chemistry from the University of Messina in 2013. He then obtained his PhD in 2017 under the joint supervision of Prof. Alberto Credi and Dr. Nathan McClenaghan (University of Bordeaux) within the framework of the Vinci Programme of the Università Italo-Francese, working on luminescent semiconductor nanocrystals quantum dots. He is currently a postdoctoral fellow in the Credi group.



**Serena Silvi** got her MSc in 2002 at the University of Bologna with Prof. Vincenzo Balzani and in 2006 she earned her PhD under the supervision of Prof. Alberto Credi. Since 2008 she is assistant professor at the Chemistry Department "Giacomo Ciamician" of the University of Bologna. Her research is focused on the design and characterization of artificial molecular machines and complex systems for signal processing.



**Alberto Credi** is professor of Chemistry at the University of Bologna and director of the Center for Light Activated Nanostructures (CLAN), a University-National Research Council joint laboratory for research in photochemistry, supramolecular chemistry, materials science and nanoscience. He has co-authored 4 books and over 270 scientific publications, and he is the PI of an ERC Advanced Grant for the development of light driven molecular motors.

place at interfaces, on surfaces and in the solid state. It is therefore not surprising that the growth of the field of stimuli-responsive molecular systems and materials is strictly related to the progress of research on molecular switches.<sup>[25]</sup>

This short review is aimed at illustrating recent research progresses on the design, synthesis and investigation of artificial molecular-scale devices, machines and materials that respond to light stimuli. After a short tutorial-style discussion of the photoinduced processes that can be exploited to implement light-triggered functionalities in molecular and supramolecular systems, we will describe a few selected examples taken from our work of the past five years. Potential applications, limitations and future directions are also discussed.

## 2. Photoinduced Processes in Molecular and Supramolecular Systems

Before describing specific examples it is worthwhile recalling a few basic aspects of the interaction between molecular and supramolecular systems, and light. For a more detailed discussion, the book referred here<sup>[26]</sup> can be consulted.

### 2.1 Molecular Photophysics and Photochemistry

The schematic electronic energy-level diagram for a generic molecule, that could also be a component of a supramolecular species, is shown in Figure 1. In most cases the molecule ground state is a singlet state ( $S_0$ ), and the excited states have either singlet ( $S_1$ ,  $S_2, \dots$ ) or triplet ( $T_1$ ,  $T_2, \dots$ ) nature. In principle, transitions between states having the same spin label are allowed, and those between states of different spin are forbidden. Hence, the absorption bands observed in the UV-Visible spectrum of molecules usually correspond to  $S_0 \rightarrow S_n$  transitions.

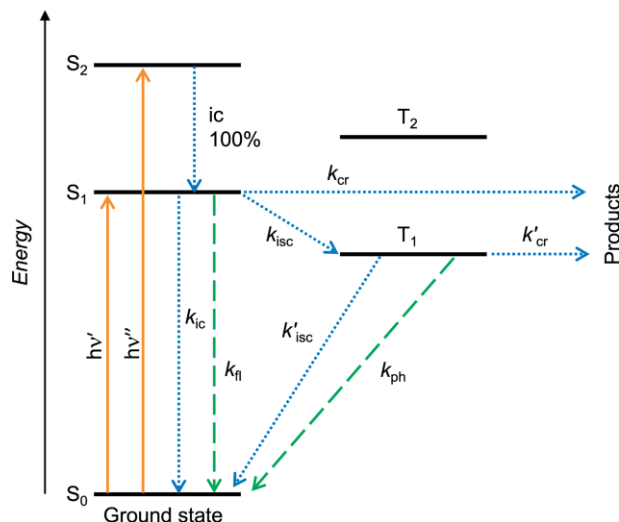


Figure 1. Schematic diagram of the electronic energy levels of a molecule and of the transitions between them: full line, absorption; dashed lines, radiative decays; dotted lines, non-radiative decays. See the text for details.

Generally speaking, the excited state obtained upon absorption of a photon is an unstable species that quickly disappears by intramolecular processes characterized by first-order kinetics.

These processes include radiative and non-radiative deactivations to lower-lying electronic states, and chemical reactions (e.g., dissociation, isomerization). When a molecule is excited to upper singlet excited states (e.g.,  $S_2$  in Figure 1), it usually undergoes a fast and unit-efficient non-radiative decay to the lowest excited singlet,  $S_1$  (internal conversion, ic). The excited molecule then evolves from the  $S_1$  state via four competing processes: non-radiative decay to the ground state (internal conversion, rate constant  $k_{ic}$ ), radiative decay to the ground state (fluorescence,  $k_{fl}$ ), conversion to the lowest triplet excited state  $T_1$  (intersystem crossing,  $k_{isc}$ ), and transformation into another species (chemical reaction,  $k_{cr}$ ). The case of the photoreaction, which is particularly relevant for the examples illustrated in the following, will be discussed in Section 2.3.

In its turn,  $T_1$  can eventually decay via non-radiative (intersystem crossing,  $k'_{isc}$ ) or radiative (phosphorescence,  $k_{ph}$ ) processes to the ground state  $S_0$ ; alternatively, it can also undergo a chemical transformation ( $k'_{cr}$ ). When the molecule contains heavy atoms, the formally spin-forbidden intersystem crossing and phosphorescence processes become faster. The lifetime  $\tau$  of the excited state, that is, the time needed to reduce its concentration by 2.718, corresponds to the reciprocal of the summation of the decay rate constants [Equation (1) and Equation (2)]:

$$\tau(S_1) = \frac{1}{k_{ic} + k_{fl} + k_{isc} + k_{cr}} \quad (1)$$

$$\tau(T_1) = \frac{1}{k_{ph} + k'_{isc} + k'_{cr}} \quad (2)$$

Typical lifetime values are comprised between  $10^{-10}$ – $10^{-7}$  s (0.1–100 ns) for  $\tau(S_1)$  and  $10^{-4}$ – $10^0$  s (0.1 ms–1 s) for  $\tau(T_1)$ . The quantum yield of fluorescence  $\Phi_{fl}$  is the number of photons emitted by  $S_1$  in a given period of time divided by the number of absorbed photons in the same period; it can be calculated with Equation (3). Similarly, the phosphorescence quantum yield  $\Phi_{ph}$  (ratio between the number of photons emitted by  $T_1$  and the number of absorbed photons) and the photoreaction quantum yields  $\Phi_{cr}$  and  $\Phi'_{cr}$  (ratio between the number of transformed molecules and the number of absorbed photons) are given by Equation (4), Equation (5) and Equation (6). Quantum yield values can range between 0 and 1. Excited state lifetimes, and fluorescence, phosphorescence and photoreaction quantum yields are known for a large number of molecules.<sup>[27]</sup>

$$\Phi_{fl} = \frac{k_{fl}}{k_{ic} + k_{fl} + k_{isc} + k_{cr}} \quad (3)$$

$$\Phi_{ph} = \frac{k_{isc}}{k_{ic} + k_{fl} + k_{isc} + k_{cr}} \times \frac{k_{ph}}{k_{ph} + k'_{isc} + k'_{cr}} \quad (4)$$

$$\Phi_{cr} = \frac{k_{cr}}{k_{ic} + k_{fl} + k_{isc} + k_{cr}} \quad (5)$$

$$\Phi'_{cr} = \frac{k_{isc}}{k_{ic} + k_{fl} + k_{isc} + k_{cr}} \times \frac{k'_{cr}}{k_{ph} + k'_{isc} + k'_{cr}} \quad (6)$$

When the intramolecular deactivation processes are not too fast (i.e., when the lifetime of the excited state is not too short), an excited molecule  $*X$  in fluid solution may have a chance to encounter a molecule of another solute,  $Y$  (Figure 2). In such a

case, specific interactions can trigger the disappearance of the excited state by second-order processes. The most important kinds of interactions in an encounter are those leading to energy transfer, electron transfer, and chemical reaction. Due to the occurrence of these processes, the intrinsic properties of  $*X$  are quenched; energy transfer also causes the sensitization of the excited state properties of  $Y$ . Simple kinetic arguments show that only the excited states with a lifetime longer than ca. 1 ns can have a reasonable chance to run into other solute molecules.

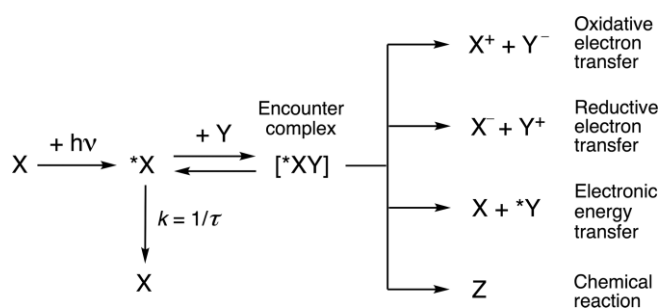


Figure 2. Bimolecular processes that could take place following an encounter between an excited molecule  $*X$  and another chemical species  $Y$ .

An in-depth discussion of the thermodynamic and kinetic aspects of energy- and electron-transfer processes is beyond the scope of this article and can be found in the literature.<sup>[28–30]</sup> Here, it is sufficient to emphasize that a molecule in an electronically excited state has quite distinct properties with respect to the same molecule in the ground state. The most significant difference is that an electronic excited state has a much higher energy content ( $>100 \text{ kJ mol}^{-1}$ ) compared to the corresponding ground state, which translates into an enhanced reactivity. The fact that a molecule in an excited state is both a stronger reductant and a stronger oxidant than in the ground state is a clear evidence of this fact.<sup>[31]</sup>

## 2.2 Supramolecular Photochemistry

Molecular components can be arranged in a supramolecular system so as to favour the occurrence of bimolecular processes, such as energy- and electron-transfer processes, and chemical reactions. Indeed, the component to be excited,  $X$ , can be placed in the vicinity of a suitable molecule,  $Y$ , in the supramolecular assembly.

Let us consider the simple case of an  $X\cdots Y$  supramolecular system, where  $X$  is the light-absorbing molecular unit [Equation (7)], and  $Y$  is the other molecular component involved with  $X$  in the photoinduced process. The symbol  $\cdots$  denotes the chemical bond that keeps  $X$  and  $Y$  together, which can vary from weak Van der Waals interactions to the limit of strong covalent bonds (provided that they do not radically perturb the nature of the  $X$  and  $Y$  components in the complex). In such a system, after light excitation of  $X$  there is no need to wait for a diffusion controlled encounter between  $*X$  and  $Y$ , as in molecular photochemistry, because the two reaction partners can already be at an interaction distance suitable for energy transfer [Equation (8)], electron transfer [Equation (9) and Equation (10)] or chemical reaction [Equation (11)]:

tion (8)], electron transfer [Equation (9) and Equation (10)] or chemical reaction [Equation (11)]:



Photoinduced energy transfer [Equation (7) and Equation (8)] is followed by radiative and/or non-radiative deactivation of the excited acceptor [Equation (12)]. Another possibility, which however requires special conditions – primarily, that the excited levels of the donor and acceptor units are very close in energy – is reverse energy transfer from the sensitized  $*Y$  to  $X$  [Equation (13)]. In such a case, delayed luminescence of the  $X$  component can be observed if  $*X$  undergoes radiative decay.<sup>[32]</sup> In the absence of rapid chemical transformations of the oxidized and/or reduced species, after photoinduced electron transfer [Equation (7), Equation (9) and Equation (10)] the starting ground state is regenerated by spontaneous back electron-transfer processes [Equation (14) and Equation (15)]:



In supramolecular complexes, energy- and electron-transfer processes follow first-order kinetics and do not rely on diffusion of the partners. Hence, in suitably designed supramolecular systems even very short lived excited states can become involved in such processes.

## 2.3 Photochemical Reactions

As discussed in Section 2.1, electronically excited states can decay by undergoing a chemical transformation, either intramolecularly (i.e., with first-order kinetics, Figure 1) or via a bimolecular encounter with another ground-state reactant (Figure 2). Here, we will briefly recall only a few classes of photoreactions that are relevant for the examples presented in the next Sections. Readers interested in a more thorough discussion of organic and inorganic photoreactions should consult these references.<sup>[33,34]</sup>

A most common and widely investigated class of unimolecular light-induced reactions is photoisomerization. It refers to the transformation of a compound from one isomeric form to another as a consequence of light irradiation. As the different forms usually have different absorption spectra, this phenomenon is also known as photochromism.<sup>[35]</sup> In most instances, the interconvertible forms are configurational stereoisomers (e.g.,  $E$ - $Z$ ) or open- and closed-ring isomers. Azobenzene, stilbene, hydrazone and chalcone derivatives provide examples of configurational photoisomerization, while diarylethenes, fulgides, spiropyrans and dihydroazulenes undergo ring closing and opening phototransformations. The light-generated isomer can

either revert thermally to the initial form (thermally reversible photochromes, or T-type), or be inert even at high temperature; in the latter case the back reaction must be promoted by light (photochemically reversible photochromes, or P-type). Spiropyrans and diarylethenes are examples of T-type and P-type photochromes, respectively.

A prototypical case of T-type photoisomerization is the *E-Z* interconversion of the  $-N=N-$  double bond in azobenzene (Figure 3). The *E* isomer is thermodynamically stable and can be transformed into the *Z* form by light irradiation; back conversion to the *E* isomer can be achieved by either light irradiation or heating. The two forms show significantly different structure and physicochemical properties, and their reversible interconversion is efficient, clean and fast. The *E-Z* photoisomerization of azobenzene is therefore an ideal reaction to implement light-driven functions within (supra)molecular systems and materials.<sup>[36]</sup> Indeed, the first examples of molecular machines, reported in the early 80s, exploited the photoisomerization of azobenzene to operate molecular tweezers,<sup>[37]</sup> in more recent years the evolution of this idea has led to the realization of highly sophisticated devices.<sup>[38]</sup> It should be recalled that, because the absorption spectra of *E*- and *Z*-azobenzene are extensively overlapped, the irradiation of either isomer leads to photostationary states in which the degree of isomerization is often far from 100%. Although such a behaviour prevents the clean and complete photoswitching between the two isomeric forms, it can lead to interesting light-induced features, as it will be discussed in Section 3.4.

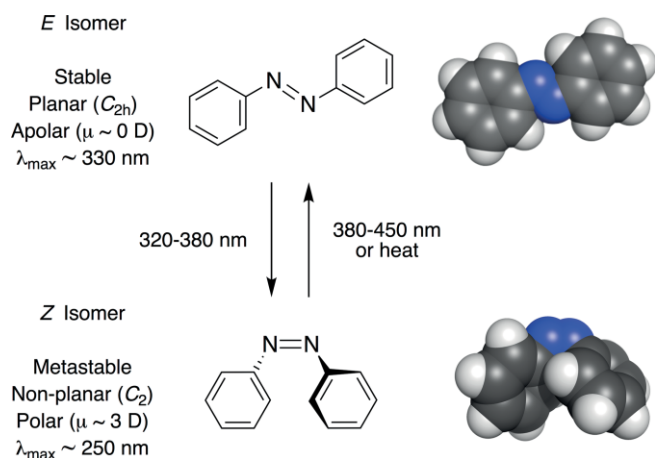


Figure 3. The *E* and *Z* configurational isomers of azobenzene, and their photochemically and thermally induced interconversion.

Photoinduced decomposition of coordination compounds is another class of unimolecular photoreactions, in which one or more ligands are detached from a metal centre as a result of light excitation.<sup>[34]</sup> A prototypical case is represented by octahedrally distorted  $Ru^{II}$  complexes such as  $[Ru(tpy)(bpy)L]^{2+}$  (*bpy* = 2,2'-bipyridine; *tpy* = 2,2':6',2''-terpyridine, *L* = monodentate ligand) (Figure 4).<sup>[39]</sup> In general,  $Ru^{II}$  polypyridine complexes show an intense metal-to-ligand charge-transfer (MLCT) absorption band in the visible region ( $\lambda_{max}$  at around 450 nm); the lowest excited state,  $^3MLCT$ , is reached with unitary efficiency from the upper lying excited states. Another metal-

centred (d-d) triplet excited state ( $^3MC$ ) lies at higher energies but it cannot be directly populated by light absorption. In  $[Ru(tpy)(bpy)L]^{2+}$ -type complexes, however, the ligand field is weak because of the structural distortion, and the  $^3MC$  is lowered in energy such that it can be thermally populated from the  $^3MLCT$  state which, as discussed above, is efficiently obtained by excitation with visible light. As the  $^3MC$  state is strongly dissociative, light irradiation in these complexes can lead to the decooordination of the non-chelating ligand (Figure 4).

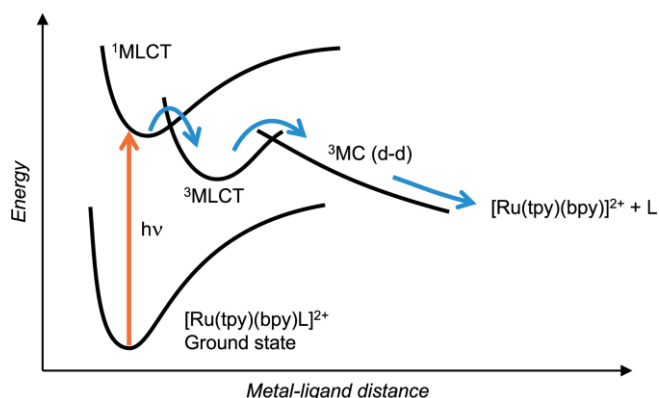
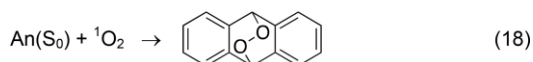
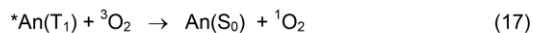


Figure 4. Potential energy diagram for a distorted octahedral complex  $[Ru(tpy)(bpy)L]^{2+}$ , showing the photoinduced expulsion of the monodentate ligand *L* as a result of the thermal population of the dissociative  $^3MC$  level from the  $^3MLCT$  state. Reproduced by permission from ref.<sup>[40]</sup>

Important classes of bimolecular photoreactions are photooxygenations and photocycloadditions. In the first case, molecular oxygen is covalently incorporated in the product as a result of light excitation. In most instances, excited singlet oxygen ( $^1O_2$ ) – generated by energy transfer from the  $T_1$  excited state of the reactant to ground state oxygen ( $^3O_2$ ) – attacks the reactant itself in the ground state. The direct reaction of the photoexcited species with ground state oxygen is also possible. A well known example of photooxygenation is the UV irradiation of an air equilibrated solution of anthracene (An), with formation of anthracene-9,10-endoperoxide. UV Excitation of anthracene affords the  $S_1$  state, which in its turn produces the  $T_1$  state by intersystem crossing [Equation (16)]; quenching of  $T_1$  by dissolved molecular oxygen generates  $^1O_2$  [Equation (17)], which subsequently attacks anthracene to yield the endoperoxide [Equation (18)].



In photocycloaddition reactions, two unsaturated molecules are joined together with the aid of light, forming a cyclic product. Anthracene provides again a common and widely investigated reaction of this kind; that is, the  $[4\pi + 4\pi]$  photocycloaddition, which leads to dimerization [Equation (19)].<sup>[41]</sup> The reaction occurs in deoxygenated solution (to avoid photooxygenation, see above), and experimental evidence indicates that the reaction proceeds via the excited singlet state.

### 3. Examples

#### 3.1 Photochemical Trapping and Release of Singlet Oxygen

Excited singlet oxygen is a strongly oxidizing species, and its controlled trapping and release is of interest for many applications in materials science, wastewater treatment, optical imaging, and medical therapy.<sup>[42]</sup> As discussed in Section 2.3,  $^1\text{O}_2$  can be trapped by reaction with aromatic compounds and, in some cases, it can be thermally released. An elegant strategy to regulate the concentration of  $^1\text{O}_2$  involves the use of molecular switches.<sup>[25]</sup>

The dimethyldihydropyrene-cyclophanediene (DHP-CPD) photochromic couple shown in Figure 5 (compounds **1** and **2**) belongs to the family of diarylethenes.<sup>[43]</sup> In deoxygenated acetonitrile, visible-light irradiation of the colored form **1** affords the colorless CPD isomer **2**; the reverse conversion (**2**→**1**) is accomplished either by UV irradiation or thermally. When the irradiation is performed on an air-equilibrated solution, the colorless endoperoxide **2-O<sub>2</sub>** – formally obtained by addition of one dioxygen molecule to the open form **2** – is quantitatively obtained (Figure 5).

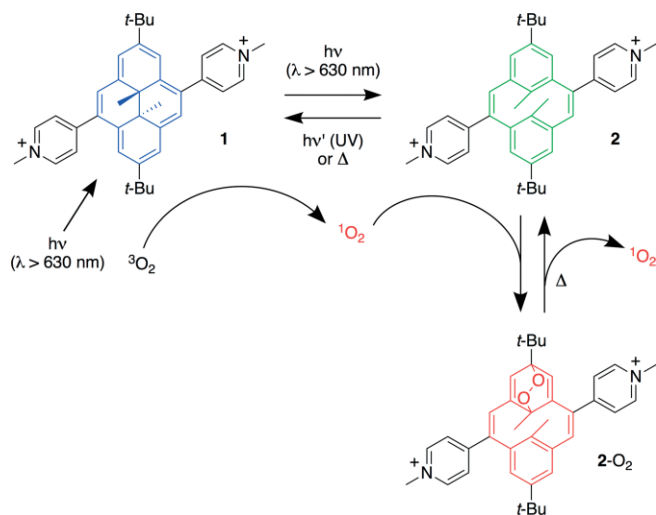
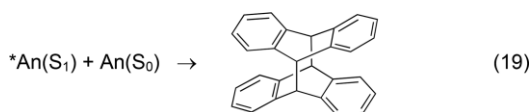


Figure 5. The photochemical and thermal interconversion processes between dihydropyrene **1**, cyclophanediene **2**, and endoperoxide **2-O<sub>2</sub>**.

These results can be rationalized as follows. Visible irradiation of the starting isomer **1** in the ground state ( $S_0$ ) produces its singlet excited state ( $S_1$ ) which isomerizes to **2**. The  $S_1$  level of **1** can also decay to the triplet state  $T_1$  by intersystem crossing. As  $T_1$  is efficiently quenched by  $\text{O}_2$ , **1** can play the role of oxygen sensitizer. The photogenerated singlet oxygen then reacts with **2** to afford the endoperoxide **2-O<sub>2</sub>**. It should be pointed out that **2** does not absorb the irradiation light and does not react with ground-state oxygen  $^3\text{O}_2$  under dark conditions.



The endoperoxide **2-O<sub>2</sub>** first releases the trapped dioxygen molecule to form the cyclophanediene species **2**, which then thermally reverts to the initial DHP isomer **1** without degradation or formation of rearrangement products (Figure 5).  $\text{O}_2$  is released in its singlet excited state, as evidenced by EPR and NMR trapping experiments, with nearly quantitative efficiency. The thermal release of  $^1\text{O}_2$  can be directly monitored by following the time-dependent decay of its phosphorescence emission in the near infrared (1270 nm), which is observed in the absence of photoexcitation (Figure 6).

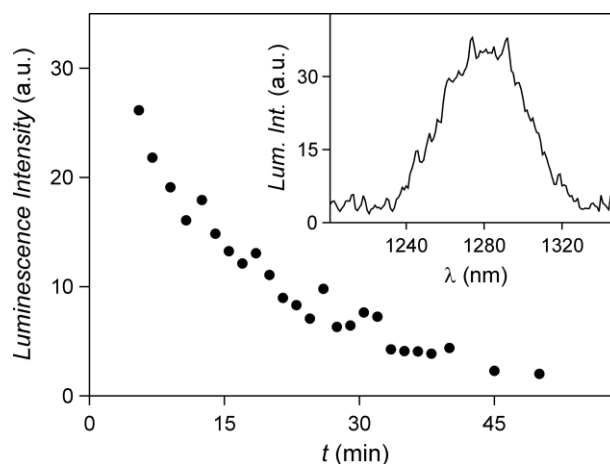


Figure 6. Time-dependent luminescence intensity changes at 1270 nm observed for **2-O<sub>2</sub>** (0.19 mM), obtained in situ upon exhaustive irradiation of **1** with visible light. The emission spectrum of the same solution (inset) shows the characteristic phosphorescence band of  $^1\text{O}_2$ . All these measurements were performed without photoexcitation. Conditions:  $\text{CD}_3\text{CN}$ , 0.19 mM, 60 °C. Reproduced by permission from ref.<sup>[43]</sup>

Considering that the generation of endoperoxide from plain dimethyldihydropyrene proceeds with low yields, the high efficiency of the photooxygenation from **1** highlights the importance of the electron withdrawing pyridinium substituents on the oxygen trapping/releasing process. This system combines together several important practical features: (i) it does not require an external  $^1\text{O}_2$  photosensitizer, (ii) it uses low energy (red) light, (iii) it exhibits excellent reversibility, and (iv) its properties can be tuned by modification of its substitution pattern. For example, the peripheral methyl groups could be replaced by functional moieties such as reactive groups or polyether chains, thus enabling the preparation of advanced materials or the adjustment of the solubility of the compounds.

#### 3.2 Photochemically Driven Change of Molecular Topology

Rotaxanes and catenanes are two major classes of mechanically interlocked molecules (MIMs),<sup>[44,45]</sup> which are interesting not only because of their topology, but also because they are appealing for the realization of nanoscale devices and machines.<sup>[8–15,45]</sup> Examples of topology interconversion from one class of MIM (e.g. from rotaxane to catenane) to another are rare.

Recently, we described the synthesis and characterisation of the [2]rotaxane **3** (Figure 7), and studied its photochemical conversion to a well-defined catenane product, concomitant fluo-

rescence switching, and thermal and photochemical return to the original rotaxane structure.<sup>[46]</sup>

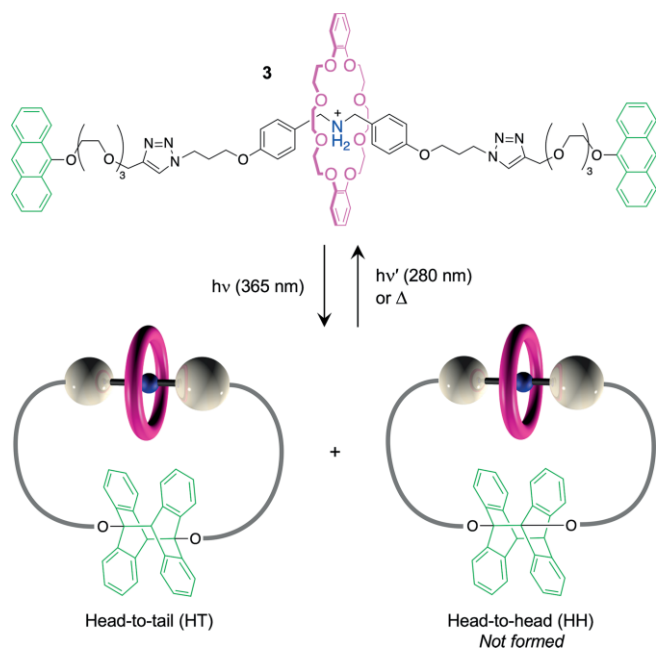


Figure 7. Structure formula of the [2]rotaxane **3** and the two catenated regioisomers (antiparallel, HT, and parallel, HH) that can be formed by the  $[4\pi + 4\pi]$  photocycloaddition of the anthracene-based stoppers. The experimental data suggest that only the HT isomer is obtained.

The rotaxane consists of an axle component that comprises a central dibenzylammonium unit and 9-alkoxyanthracene stoppers, threaded through a dibenzo[24]crown-8 (DB24C8) macrocycle. The intramolecular photodimerization of the terminal anthracene units of **3** would cause the rotaxane-to-catenane transformation. Anthracene moieties functionalized at the 9-position are employed as the photoactive unit in order to limit the number of photoproduct regioisomers to a stable antiparallel head-to-tail isomer (HT), and an unstable head-to-head isomer (HH).

Irradiation of **3** at 365 nm in degassed acetonitrile affords the virtually complete conversion into the photodimerized catenane product, with a quantum yield of 0.14. The high efficiency of the photoreaction in dilute solution and its independence on concentration (up to mM values) confirms its intramolecular character. The relatively high thermal stability of the photodimer suggests the formation of the HT isomer. The original rotaxane could be quantitatively restored either upon heating the catenane to 120 °C, or by irradiation at 280 nm, where the photodimer exhibits its absorption maximum. The reversible rotaxane-catenane photoconversion is accompanied by the quenching and revival of the anthracene-type fluorescence in the 400–530 nm region.

### 3.3 A Molecular Scale Transporter

The directed transport of substrates within cells is a key function of biomolecular machines. The construction of synthetic molecular machines that can transport molecular or ionic spe-

cies in a controlled manner is a challenging goal in nanoscience, and can form the basis for novel approaches in catalysis, materials science, energy conversion and medical therapy.<sup>[8–15]</sup>

The recently reported multicomponent rotaxane **4** (Figure 8) possesses all the structural and functional elements required to perform controlled and directed transport of a molecular cargo.<sup>[47]</sup> The rotaxane consists of a DB24C8-type ring interlocked with an axle component that comprises two recognition sites, namely a dibenzylammonium and a 4,4-bipyridinium units. The macrocycle is endowed with a short tether terminated with a nitrile group that serves as an anchor for the cargo.

<sup>1</sup>H NMR Spectra and electrochemical studies indicate that in acetone solution the ring of **4** encircles the ammonium site, in line with earlier investigations on similar systems.<sup>[8,48]</sup> Upon addition of one equivalent of phosphazene base, the ammonium unit of the rotaxane is quantitatively deprotonated and the ring shifts on the bipyridinium site. The successive addition of a stoichiometric amount of acid regenerates the ammonium site of **4** and the ring returns to the original position. Hence, rotaxane **4** behaves as a reversible molecular shuttle driven by pH changes.<sup>[49]</sup>

The cargo loading-unloading process is based on the photochemical ligand decoordination and thermal recoordination in suitable Ru<sup>II</sup> polypyridine complexes. As anticipated in Section 2.3, in distorted octahedral complexes such as  $[\text{Ru}(\text{tpy})(\text{bpy})\text{L}]^{2+}$ , irradiation with visible light causes the selective detachment of the monodentate ligand and its replacement by solvent molecules or other ligands (Figure 4).<sup>[39]</sup> The thermally driven recoordination of the expelled ligand may successively take place in the dark.

The cargo-loaded molecular transporter **4·5** (Figure 8) was obtained by reacting  $[\text{Ru}(\text{bpy})(\text{tpy})(\text{CH}_3\text{CN})]^{2+}$ , **5**·CH<sub>3</sub>CN, with rotaxane **4** in acetone. <sup>1</sup>H NMR and voltammetric measurements confirm that in the loaded transporter **4·5** the macrocycle encircles the ammonium site, and the Ru-based cargo is bound to the ring via the nitrile-terminated tether. The addition of one equivalent of base triggers the quantitative displacement of the crown ether onto the bipyridinium station, with no effect on the attached cargo. At this point, upon irradiation with visible light the cargo **5** is fully detached and released in the solution. The successive addition of acid regenerates the ammonium site and the (unloaded) ring returns on its starting position (Figure 8). While the thermal recoordination of **5** to **4** in a 1:1 ratio can be achieved with 30 % yield, the thermally driven reloading in situ after the full transporting cycle is not observed. It is likely that the coordination position on the Ru<sup>II</sup> ion available after photodissociation is filled by adventitious water molecules or anions, and thus **5** is no longer available for recoordination to **4**.

In spite of the lack of reversibility in situ and the close proximity of the two stations on the axle, which limits the distance travelled by the cargo, the molecular transporter fulfils several non-trivial requirements. First, the ring displacement-return and the cargo loading-unloading reactions are reversible, independent from one another, and controlled by orthogonal stimuli (pH changes and light, respectively). Another significant feature is

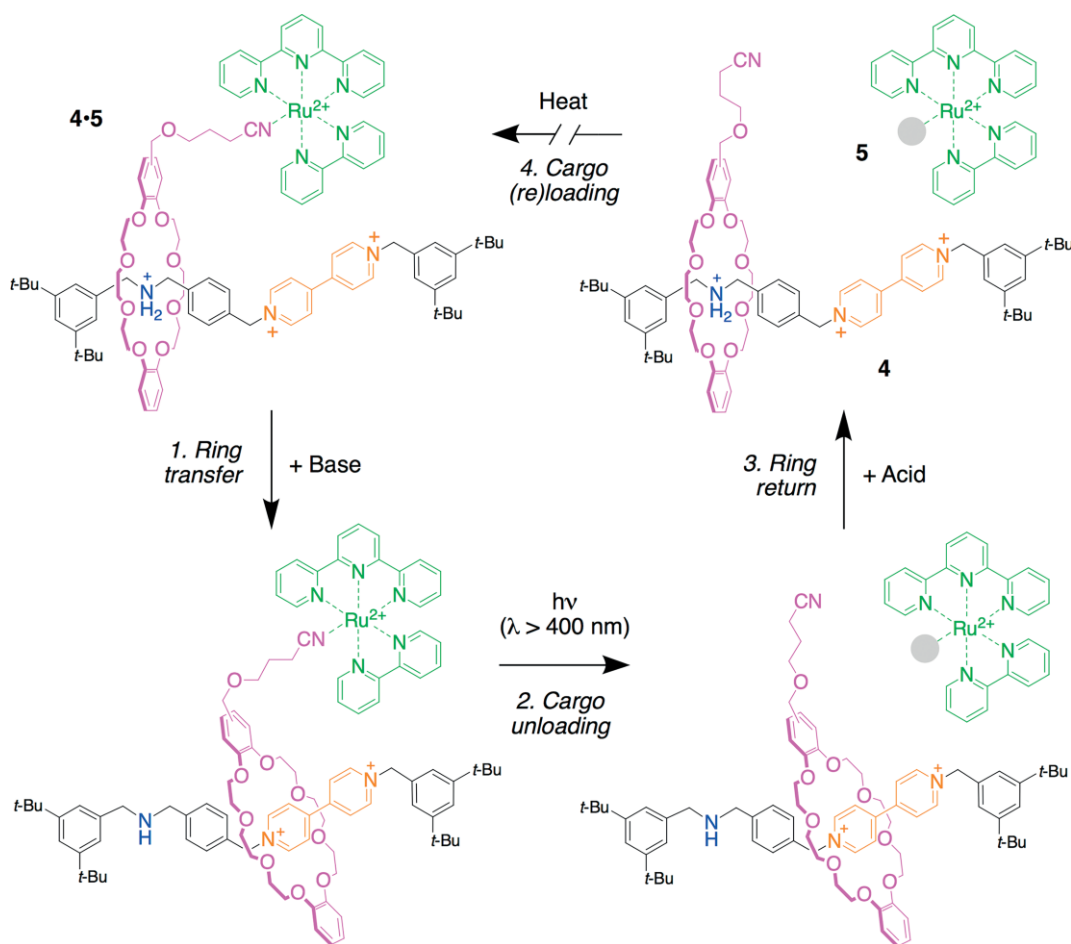


Figure 8. Structure formula of the molecular shuttle **4** loaded with cargo **5** and schematic representation of its operation as a nanoscale transporter. The grey spheres represent solvent molecules or other adventitious ligands.

that, because of the kinetically inert coordination bond, the cargo remains attached to the machine during the shuttling. Clearly, to take full advantage of the directional control of the transport the molecular "track" would need to be immobilized in some way, e.g., deposited on a surface, embedded in a polymer or inserted in a membrane.

### 3.4 Light-Activated Supramolecular Pumps

Investigations on stimuli-controlled threading and dethreading of ring and axle molecular components to yield and disassemble pseudorotaxanes (Figure 9a) have been instrumental for the development of molecular machines based on MIMs.<sup>[8–15,45]</sup> While these studies are nowadays well established, gaining control on the threading-dethreading direction of an oriented axle with respect to the ring (Figure 9b) remains an intriguing challenge.<sup>[50,51]</sup> The design and construction of pseudorotaxanes exhibiting stimuli-controlled relative unidirectional threading and dethreading movements is indeed a first key step forward towards the realization of artificial molecular pumps, as well as of linear motors based on rotaxanes and rotary motors based on catenanes (Figure 9c,d).<sup>[52]</sup>

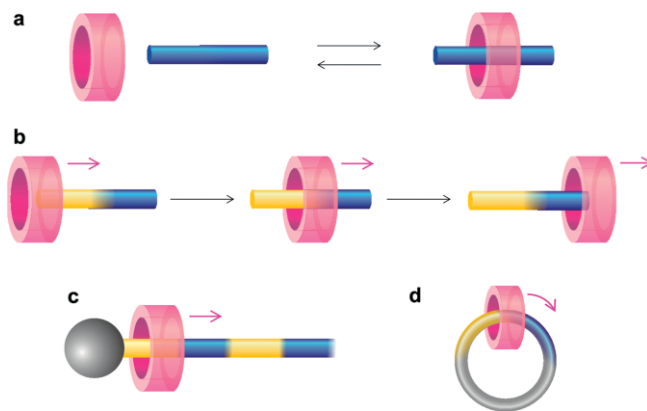


Figure 9. Schematic representation of the threading/dethreading of a pseudorotaxane (a) and of the relative unidirectional transit of a macrocycle along a nonsymmetric molecular axle (b). By incorporating the system shown in (b) in a rotaxane or a catenane, linear or rotary motors may be obtained, respectively (c). Adapted by permission from ref.<sup>[52]</sup>

A few years ago we discovered that the assembly between dibenzylammonium-type ions and DB24C8 can be controlled thermodynamically and kinetically by changing the configuration of azobenzene units appended to the extremities of the

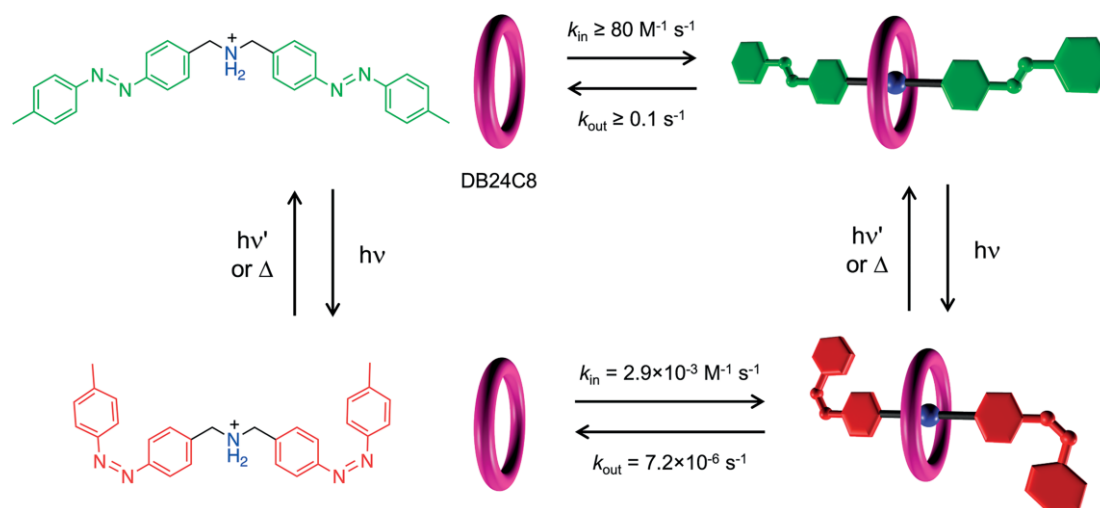


Figure 10. Representation of the self-assembly equilibria (horizontal processes) and photoisomerization (vertical processes) involving an azobenzene-containing secondary ammonium axle and the DB24C8 ring (acetonitrile, 298 K).

secondary ammonium axle (Figure 10).<sup>[53,54]</sup> In particular, the  $E \rightarrow Z$  photoisomerization of the terminal azobenzenes causes (i) a destabilization of the pseudorotaxane complex, and (ii) a huge decrease in the threading-dethreading rate constants. In summary, azobenzene behaves as a photoswitchable destabilizing agent and blocking group for the assembly of the ring with the axle; these effects are fully reversible on account of the reversibility of the  $E$ - $Z$  isomerization.

With these pieces of information in hand, the oriented axle component **6** (Figure 11) was designed and synthesized to achieve the light powered directionally controlled transit of a crown ether macrocycle.<sup>[55]</sup> Compound **6** comprises a central secondary ammonium recognition site (Amm), functionalized with an azobenzene unit (Azo) on one side and a non-photoactive cyclopentyl moiety (Cp) on the other side. The macrocycle is the crown ether ring **7**, obtained by replacing the benzene moieties of DB24C8 with naphthalene units. It should be noted that the ring can slip over the Cp unit, but with a rate that is nearly two orders of magnitude smaller than that for the Azo unit at room temp.

In  $\text{CH}_2\text{Cl}_2$  solution at room temperature, the efficient self-assembly of a pseudorotaxane is obtained, with **7** encircling the ammonium site of  $E$ -**6** on account of hydrogen bonding interactions. The experiments show that, as anticipated in the previous paragraph, the  $E$ -Azo extremity of the axle exhibits a significantly smaller hindrance than the Cp end for the passage of the macrocycle; such a marked kinetic preference thus dictates the direction of the first threading step.

The absorption of a UV or blue photon triggers the isomerization of the Azo-end to the  $Z$  isomer. As pointed out earlier, such a transformation has two crucial consequences: (i) the pseudorotaxane is destabilized, and (ii) the threading barrier at the  $Z$ -Azo end is substantially increased, making the Cp end the kinetically preferred extremity for the passage of the ring. As a result, a fraction of the complexes in a population must dethread, with the rings escaping from the Cp end (Figure 11b). Because both isomers of azobenzene are photoreactive and absorb in the same spectral region, another photon, identical to

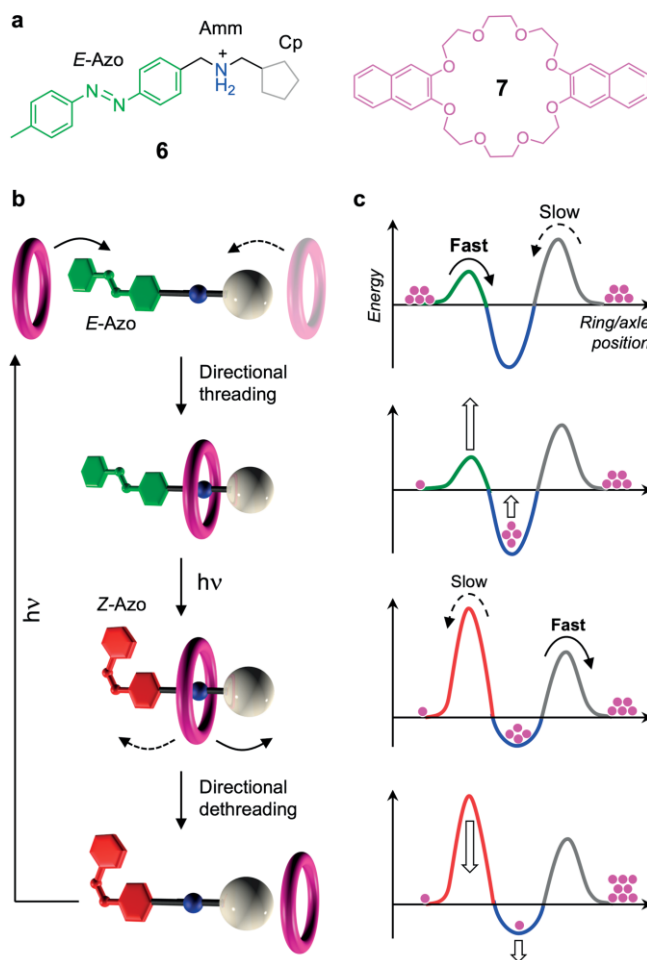


Figure 11. (a) Structure formula of the axle **6** and ring **7**, the components of a photochemical autonomous supramolecular pump. (b) Operation mechanism of the relative unidirectional transit of the ring along the axle, driven by light. (c) Simplified potential energy profiles as a function of the ring-axle relative position for each structure shown in (b). Dashed lines denote processes that are too slow to take place. Adapted by permission from ref.<sup>[20]</sup>

the first one, can trigger the transformation of **Z-6** back to **E-6**, thereby completing the operation cycle (Figure 11b). Directional threading of **E-6** and **7** can occur again, and the process can be repeated by absorption of another two photons.<sup>[56]</sup>

The ability of the machine to repeat its working cycle under constant conditions as long as the energy source (in this case, photons) is on – i.e., autonomous operation – is common for biomolecular machines,<sup>[18]</sup> but it is a rare and valuable feature for synthetic ones.<sup>[8–11,57]</sup> Therefore, what makes azobenzene a poor switch, because it prevents a complete conversion between the isomers (see Section 2.3), becomes an important advantage, as it enables autonomous cycling.

As shown in Figure 11c, the system uses photons to achieve a periodic modulation of the ring-axle energy profile (i.e., ratcheting),<sup>[11]</sup> and is thus able to convert Brownian fluctuations into directed motion. It can operate continuously under photo-stationary conditions, that is, under the effect of a single optical stimulus with constant wavelength and intensity. Remarkably, our experiments clearly show that the self-assembly reactions are shifted away from equilibrium under photoirradiation, a situation that persists as long as the light is on. Hence, this device is a unique example of a dissipative self-assembling system, and the first and sole autonomous artificial molecular pump reported to date.<sup>[58]</sup> Further valuable points are the minimalistic design, structural simplicity, stability and reversibility. A new version of the system that comprises a cyanoazobenzene unit in the axle has been recently described.<sup>[59]</sup>

### 3.5 Photoswitchable Molecular Materials Based on Azobenzene Tetramers

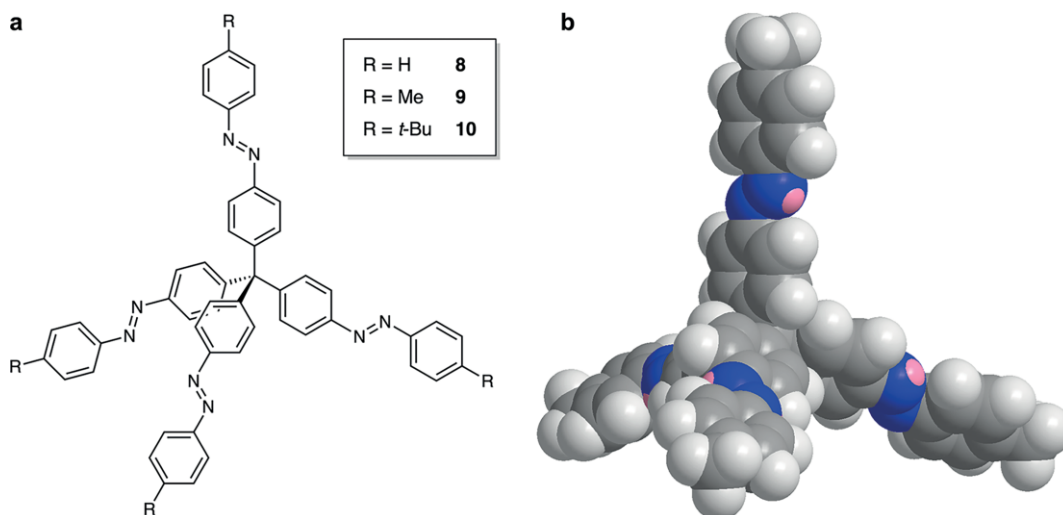
In recent years, owing to the various applications of photochromic compounds in science and technology, photoisomerization in the crystalline solid state has been attracting much interest.<sup>[60,61]</sup> Diarylethenes, for instance, undergo highly efficient and reversible single crystal-to-single crystal photoisomerization, which has been exploited to obtain intriguing photomechanical effects.<sup>[60,62]</sup> Conversely, the *E-Z* photoisomerization of

azobenzenes, because of the relatively large structural change of the molecule, is difficult to achieve in the densely packed crystalline state.

Recently we reported the synthesis, structural determination, and reversible photoisomerization in solution and in the solid state of three shape-persistent tetra(azobenzene)methane derivatives.<sup>[63]</sup> These species (compounds **EEEE-8–10**, Figure 12a) consist of four *E*-azobenzene units covalently linked to a tetrahedral carbon atom, and bear different peripheral substituents – H, Me or *t*Bu – in the *para* position of each azobenzene moiety. Because of the rigid tetrahedral shape of the molecule and its stiff, extended branches (Figure 12b) that hamper a tightly packed arrangement, it could be hypothesized that a porous crystal structure may be obtained, and that the photoinduced isomerization of the azobenzene units could be observed in the solid state, owing to the available free volume and weak intermolecular interactions. Porous molecular crystals can indeed outperform metal-organic and covalent frameworks in terms of preparation, processing, structural modulation and functional flexibility.<sup>[64]</sup>

In solution, compounds **8–10** show similar spectroscopic and photochemical properties, and the behaviour of **10** (*R* = *t*Bu) will be discussed as a representative case. Irradiation of the **EEEE-10** at 365 nm causes the *E*→*Z* isomerization, as indicated by the absorption spectral changes. The facts that isobestic points are not maintained, and the photoisomerization quantum yield decreases throughout the irradiation, suggests that the four azobenzene units are not electronically independent. Exhaustive irradiation of **10** in C<sub>6</sub>D<sub>6</sub> at 365 nm affords a photo-stationary state with an overall *E*→*Z* conversion of 97 %, that consists of 89 % **ZZZZ**, 6 % **EZZZ**, 3 % **EEZZ**, <1 % **EEEE** and <1 % **EEEE**.

The all-*E* isomers of **8–10** yield tetragonal crystals wherein an efficient molecular packing is frustrated because of the rigid tetrahedral arrangement of the *E*-azobenzene units. The packing is rendered even more difficult by the presence of bulky peripheral substituents, as in the case of **10**. The crystals of **EEEE-10** (Figure 13a) and **EEEE-9** exhibit empty channels and a



free volume of 10.4 % and 8.1 %, respectively. In the case of *EEEE*-**8** the empty space (6.7 %) corresponds to discrete and unconnected regions (Figure 13b). It is important to remark that the extrinsic porosity exhibited by these molecular crystals – that is, the pores arise solely from the solid-state molecular packing and not from a concave molecular shape – is uncommon and of challenging design.<sup>[64]</sup>

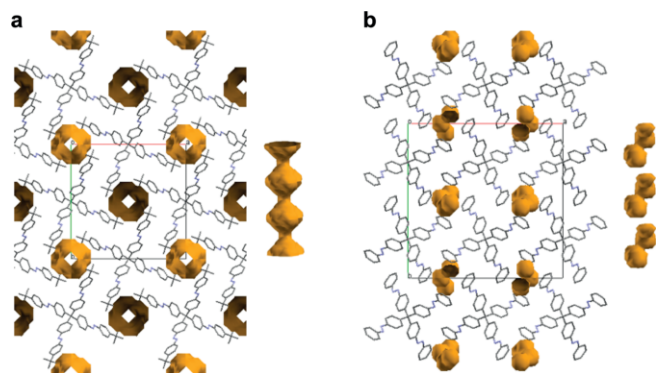


Figure 13. Stick representation of the crystal structure of the all-*E* isomers of **10** (a) and **8** (b) and space filling view of the inner voids. The side view of the pores (channels for **10**, non-communicating cavities for **8**) is displayed in the right part of each panel. Hydrogen atoms are omitted for clarity.

Crystalline powders of **8–10** in the all-*E* form deposited on quartz slides, were irradiated at 365 nm and investigated by X-ray powder diffraction, polarizing optical microscopy, UV-Visible absorption spectroscopy, and <sup>1</sup>H NMR spectroscopy (after dissolution in C<sub>6</sub>D<sub>6</sub>). The results show that (i) light irradiation causes an efficient *E*→*Z* isomerization (32 % *E*→*Z* conversion at the photostationary state for **10**), and (ii) the material becomes amorphous. Upon either visible irradiation or by heating of the thin solid films, the *Z*→*E* back reaction takes place. When the all-*E* form is thermally regenerated, the crystallinity is fully restored. Alternated *E*→*Z* and *Z*→*E* photoreactions can be performed many times without appreciable degradation of the films.

Remarkably, the melting point of all-*E* **10** is around 400 °C, while the amorphous material afforded by photoirradiation at

room temperature has the consistency of a viscous liquid. A similar behaviour is observed for derivatives **8** and **9**. Thus, azobenzene tetramers **8–10** undergo a *photoinduced isothermal phase transition*<sup>[65]</sup> that can be of interest for the development of light-responsive adhesives and coatings. The changes in the optical properties caused by photoisomerization of the thin films can have implications for information storage.<sup>[66]</sup> These compounds, because of their tetrapod structure which resembles that of a caltrop, are promising for probe microscopy studies upon adsorption on surfaces. Indeed, high-resolution STM experiments performed on **9** deposited on an Ag(111) surface brought about highly interesting results.<sup>[67]</sup>

Gas adsorption measurements were employed to study the porosity of the molecular crystals. While the gas uptake of *EEEE*-**8** is negligible, the all-*E* forms of both **9** and **10** show N<sub>2</sub> and CO<sub>2</sub> adsorption isotherms with Langmuir type-I profiles (Figure 14a). The remarkably large CO<sub>2</sub>/N<sub>2</sub> selectivity exhibited by these compounds (as high as 80 for *EEEE*-**9**) can be of interest for the selective capture of carbon dioxide in a mixture with N<sub>2</sub> (e.g. in flue gases). The maximum CO<sub>2</sub> uptake (52 cm<sup>3</sup> g<sup>-1</sup> for *EEEE*-**10** at 195 K and 1 bar), corresponding to the presence of two carbon dioxide molecules per cavity, is in agreement with the void as estimated from the crystallographic structure, and indicates that gas diffusion through the permeable crystal affords the complete filling of the cavities.

Conversely, solid **9** and **10** in the all-*Z* forms (prepared by precipitation from solution after exhaustive UV irradiation), exhibit a negligible gas uptake, as shown by their CO<sub>2</sub> adsorption isotherms (Figure 14b). The original Langmuir adsorption behaviour is restored by heating up the solid sample. Thus, the photoisomerization and thermal relaxation of the azobenzene moieties of **9** and **10** in the solid state enables the reversible switching between porous and non-porous materials.

At present, compounds **9–10** provide a unique example of molecular crystals whose nanoscale porosity can be switched off by light and restored by heating.<sup>[63]</sup> They represent a first step forward towards the development of solids in which the microporous structure provides the space required for the light-induced structural changes of embedded photoreactive units.

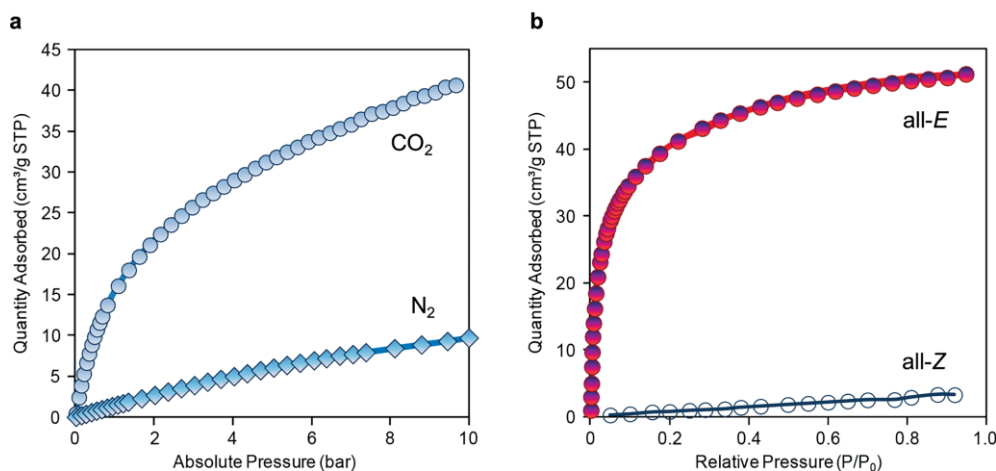


Figure 14. (a) CO<sub>2</sub> (circles) and N<sub>2</sub> (diamonds) adsorption isotherms of *EEEE*-**10** at 273 K. (b) CO<sub>2</sub> adsorption isotherms of the all-*E* (filled circles) and all-*Z* (empty circles) isomers of **10** at 195 K.

Investigations of this kind are also aimed at gaining a better understanding of photochemical reactions in the solid state and phase transitions induced by light.

### 3.6 Delayed Luminescence in Quantum Dot-Pyrene Nanohybrids

Quantum Dots (QDs) are inorganic semiconductor nanocrystals endowed with unique size-dependent physico-chemical properties.<sup>[68]</sup> CdSe QDs, in particular, exhibit an intense absorption all across the UV-Visible region, and an intense luminescence with narrow spectral dispersion whose maximum wavelength can be accurately tuned by adjusting the diameter of the nanocrystal in the nm domain.<sup>[69]</sup> By modifying the surface-capping monolayer of organic ligands, photoactive QDs can be combined with molecular chromophores,<sup>[70,71]</sup> in order to obtain QD-molecule hybrids with novel photophysical properties which can be of interest for applications in sensing, lighting and photovoltaic devices.<sup>[70,72]</sup>

We reported earlier that CdSe QDs overcoated with a ZnS shell and surface-functionalized with pyrene ligands retain the photophysical properties of the CdSe and pyrene components. Such a behaviour was exploited to develop a ratiometric luminescent sensor for O<sub>2</sub> concentration in organic solvents.<sup>[73,74]</sup> More recently it was observed that CdSe QDs lacking the ZnS shell undergo interfacial unidirectional triplet-triplet energy transfer towards surface-anchored polyaromatic carboxylic acid energy acceptors, thereby acting as photosensitizers to populate long-lived molecular triplets.<sup>[75]</sup> Energy transfer in the reverse direction, that is, from photogenerated organic triplets to interfaced PbSe and PbS QDs, was also observed.<sup>[76,77]</sup>

We hypothesized that nanoconjugates with novel photophysical properties could be obtained by fine-tuning the QD emissive level (through adjusting the nanocrystal diameter) such that it is quasi-isoenergetic with long-lived triplet states of surface-anchored organic chromophores. In such hybrids, if the intercomponent energy transfer is fast with respect to other decay pathways, reversible electronic energy transfer (REET) between chromophores may take place (Section 2.2). In analogy with molecular bichromophoric species,<sup>[32,78]</sup> this phenomenon would dramatically modify the properties of the excited QD, particularly with regard to the luminescence lifetime.

Specifically, if the triplet excited state of the surface-bound molecule is longer lived with respect to the QD exciton level, it can act as a reservoir for the excitation energy. Hence, the expected consequence of REET in the nanohybrid is an increase in the lifetime of the QD-based emission. Such an approach is extremely interesting because it would enable the preparation of QDs with the same emission maximum and bandshape but different lifetime.<sup>[79]</sup>

To show the validity of the principle,<sup>[80]</sup> we prepared a set of four CdSe QDs with different diameters (and thus different exciton energy levels) and we surface-functionalized them with 1-pyrenecarboxylic acid (1-PCA) (Figure 15).<sup>[79]</sup> Pyrene is an ideal chromophore in the present context because of its long-lived triplet state ( $\tau_T \approx 10$  ms,  $E_T = 2.1$  eV), and carboxylate groups have proven to be effective anchoring moieties to the surface of semiconductor nanoparticles.<sup>[75]</sup>

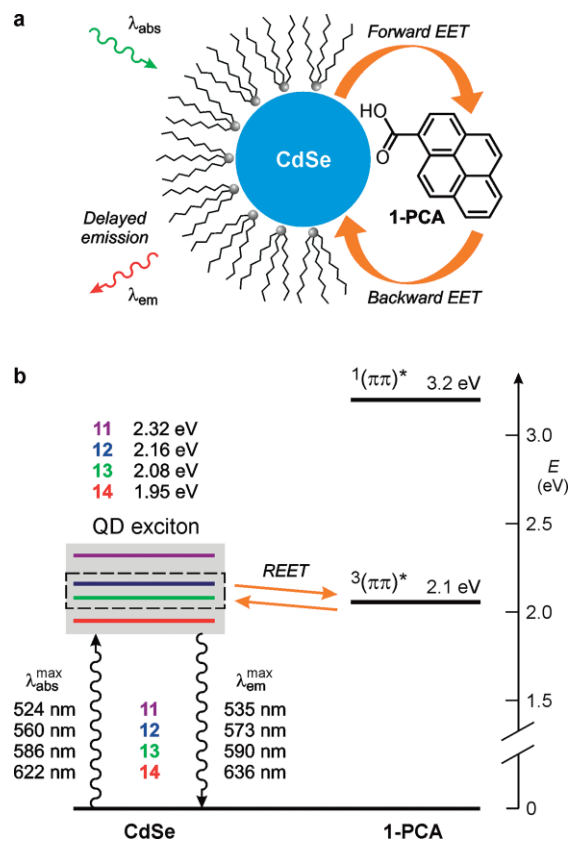


Figure 15. (a) Schematic representation of the light-induced intercomponent energy transfer processes in QD-pyrene nanohybrids. (b) Energy-level diagram for CdSe QDs decorated with 1-PCA. Samples **12** and **13** can exhibit reversible electronic energy transfer (REET) involving their exciton level and the energy-matched triplet excited state of 1-PCA. The QD exciton levels of hybrids **11** and **14** are too high and too low, respectively, for REET to occur at room temperature. Adapted by permission from ref.<sup>[79]</sup>

Four batches of hydrophobic CdSe QDs, with diameters ranging from 2.6 to 5.7 nm, were prepared and subsequently decorated with 1-PCA to afford nanohybrids **11–14** (Figure 15). The average number of pyrene units per nanocrystal depends on the size of the latter, and varies from 68 for **11** to 300 for **14**. While the presence of the pyrene chromophore does not affect the energy and profile of the QD emission in all cases, significant changes in the luminescence lifetime are seen for samples **12** and **13**.

Indeed, a component in the 100- $\mu$ s domain appears in their emission decay detected at room temperature in deoxygenated heptane (Figure 16ab). Such a long-lived component is not observed both in air-equilibrated solution (Figure 16c), in which molecular oxygen can efficiently quench the pyrene triplet state, and on the same nanocrystals of samples **12** and **13** not subjected to functionalization with 1-PCA. Remarkably, the presence of 1-PCA in nanohybrids **11** and **14**, characterized by an energy mismatch between the QD exciton and the pyrene triplet levels (Figure 15), does not cause changes in the emission behaviour in the absence or in the presence of O<sub>2</sub>, and a long-lived luminescence component is not observed (Figure 16d). All these results are consistent with the occurrence of REET between the nanocrystal and molecular chromophore components in hybrids **12** and **13**.

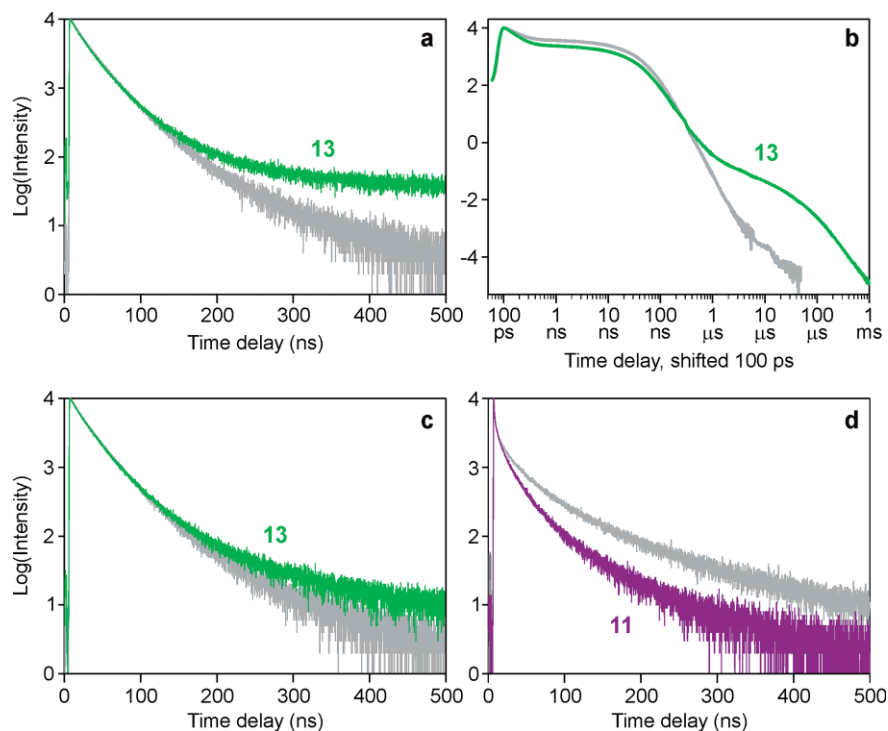


Figure 16. Luminescence decay of **13** monitored at 600 nm (green trace) in deoxygenated solution, as measured by (a) time-correlated single-photon counting (log plot,  $\lambda_{\text{exc}} = 405$  nm) and (b) gated streak camera (log-log plot,  $\lambda_{\text{exc}} = 465$  nm). (c) Luminescence decay of **13** ( $\lambda_{\text{exc}} = 405$  nm, green trace) in air equilibrated solution. (d) Luminescence decay of **11** monitored at 540 nm ( $\lambda_{\text{exc}} = 405$  nm, purple trace) in deoxygenated solution. The grey traces in all panels refer to the same experiment performed on the same QD sample lacking the 1-PCA functionalization. Conditions: heptane, room temperature. Adapted by permission from ref.<sup>[79]</sup>

This strategy enables the rational engineering of energy shuttling in QD-molecule conjugates, based on the knowledge of energy levels and decay kinetics of the constituent chromophores, on allowing their close proximity. Considering that the energy of the QD exciton can be accurately tuned by controlling its chemical composition and size, and that there is an ample choice of organic chromophores, the approach is flexible and generally applicable.

As a result, nanohybrids with long lived luminescence desirable for gated emission detection can be obtained, and QDs exhibiting the same luminescence band but different lifetimes can be designed and prepared, potentially adding a new dimension to multiplexed analyses.<sup>[71]</sup> Finally, luminescent sensing for  $\text{O}_2$  can be performed with nanocrystals that are inherently insensitive to oxygen.

#### 4. Conclusions

In the past three decades the marriage of photochemistry with supramolecular chemistry, materials science and nanoscience has triggered outstanding achievements. This research has a high scientific value because it stimulates the ingenuity of chemists and promotes cross-disciplinary interactions. Moreover, it has the potential to provide ground-breaking solutions to current pressing problems of our society: energy, environment, sustainability, and health. In this minireview we have tried to represent the progress in the field by presenting some examples taken from our most recent work.

Appropriately designed multicomponent systems endowed with photoreactive units can exhibit sophisticated functionalities under control of light, such as topology change and molecular transport. Coupling photoisomerization and self-assembly processes can lead to the realization of artificial chemical systems that can use the energy of light to operate far from chemical equilibrium, which can be extremely interesting for solar energy conversion.

While most of the systems described here operate in solution, we have shown that photoreactions can be taken advantage of also in the solid state and on single molecules adsorbed on surfaces. The photocontrol of the properties of surfaces – such as roughness and hydrophobicity – and of materials – such as density, viscosity, stiffness and porosity – may be obtained with high spatial and temporal resolution.

The studies presented here are still at an earlier stage and, despite a growing interest and an increasing effort in photochemical sciences, the research in the area continues to have a huge potential for development. Indeed, in view of the complexity of the chemical systems that can be designed and synthesized nowadays, the future of light-matter interaction promises to be extremely bright.

#### Acknowledgments

We are grateful to Guy Royal, Nathan McClenaghan, Fabrizia Grepioni and Angiolina Comotti for fruitful collaborations. We also thank Margherita Venturi for a long term and most enjoy-

able scientific interaction. Financial support from the European Research Council (ERC) under the European Union's Horizon 2020 research and innovation program (Advanced Grant "Leaps" no. 692981) and the Ministero dell'Istruzione, Università e Ricerca (FARE Grant "Ampli" no. R1659XXKX3) is gratefully acknowledged.

**Keywords:** Azobenzene · Molecular machines · Photochemistry · Quantum dots · Rotaxanes · Supramolecular chemistry

- [1] *Photobiology - The Science of Life and Light* (Ed. L. O. Björn), Springer, New York, **2008**.
- [2] V. Ramamurthy, B. Mondal, *J. Photochem. Photobiol. C* **2015**, *23*, 68.
- [3] P. Ceroni, A. Credi, M. Venturi, *Chem. Soc. Rev.* **2014**, *43*, 4068.
- [4] For a significant example, see: M. Bälter, S. Li, M. Morimoto, S. Tang, J. Hernando, G. Guirado, M. Irie, F. M. Raymo, J. Andréasson, *Chem. Sci.* **2016**, *7*, 5867.
- [5] C. Joachim, J.-P. Launay, *Nouv. J. Chim.* **1984**, *8*, 723.
- [6] V. Balzani, L. Moggi, F. Scandola, in *Supramolecular Photochemistry* (Ed. V. Balzani), Reidel, Dordrecht, **1987**, p. 1.
- [7] J.-M. Lehn, *Angew. Chem. Int. Ed. Engl.* **1988**, *27*, 89; *Angew. Chem.* **1988**, *100*, 91.
- [8] V. Balzani, A. Credi, M. Venturi, *Molecular Devices and Machines – Concepts and Perspectives for the Nanoworld*, Wiley-VCH, Weinheim, **2008**.
- [9] V. Balzani, A. Credi, F. M. Raymo, J. F. Stoddart, *Angew. Chem. Int. Ed.* **2000**, *39*, 3348; *Angew. Chem.* **2000**, *112*, 3484.
- [10] S. Erbas-Cakmak, D. A. Leigh, C. T. McTernan, A. L. Nussbaumer, *Chem. Rev.* **2015**, *115*, 10081.
- [11] S. Kassem, T. van Leeuwen, A. S. Lubbe, M. R. Wilson, B. L. Feringa, D. A. Leigh, *Chem. Soc. Rev.* **2017**, *46*, 2592.
- [12] R. D. Astumian, *Proc. Natl. Acad. Sci. USA* **10.1073/Proc. Natl. Acad. Sci. USA** **1714498115**.
- [13] A. Coskun, M. Banaszak, R. D. Astumian, J. F. Stoddart, B. A. Grzybowski, *Chem. Soc. Rev.* **2012**, *41*, 19.
- [14] E. R. Kay, D. A. Leigh, *Angew. Chem. Int. Ed.* **2015**, *54*, 10080; *Angew. Chem.* **2015**, *127*, 10218.
- [15] B. L. Feringa, *Angew. Chem. Int. Ed.* **2017**, *56*, 11060; *Angew. Chem.* **2017**, *129*, 11206.
- [16] J.-P. Sauvage, *Angew. Chem. Int. Ed.* **2017**, *56*, 11080; *Angew. Chem.* **2017**, *129*, 11228.
- [17] J. F. Stoddart, *Angew. Chem. Int. Ed.* **2017**, *56*, 11094; *Angew. Chem.* **2017**, *129*, 11244.
- [18] D. S. Goodsell, *Bionanotechnology – Lessons from Nature* Wiley, Hoboken, **2004**.
- [19] L. Zhang, V. Marcos, D. A. Leigh, *Proc. Natl. Acad. Sci. U. S. A.*, **2018**, *115*, 9397
- [20] M. Baroncini, L. Casimiro, C. de Vet, J. Groppi, S. Silvi, A. Credi, *Chemistry-Open* **2018**, *7*, 169.
- [21] See, e.g.: T. Kudernac, N. Ruangsapichat, M. Parschau, B. Maciá, N. Katsonis, S. R. Harutyunyan, K.-H. Ernst, B. L. Feringa, *Nature* **2011**, *479*, 208.
- [22] See, e.g.: J. T. Foy, Q. Li, A. Goujon, J.-R. Colard-Ilté, G. Fuks, E. Moulin, O. Schiffmann, D. Dattler, D. P. Funeriu, N. Giuseppone, *Nat. Nanotechnol.* **2017**, *12*, 540.
- [23] See, e.g.: G. De Bo, M. A. Y. Gall, S. Kuschel, J. De Winter, P. Gerbaux, D. A. Leigh, *Nat. Nanotechnol.* **2018**, *13*, 381.
- [24] See, e.g.: C. Pezzato, M. T. Nguyen, D. J. Kim, O. Anamimoghadam, L. Mosca, J. F. Stoddart, *Angew. Chem. Int. Ed.* **2018**, *57*, 9325; *Angew. Chem.* **2018**, *130*, 9469.
- [25] *Molecular Switches, Second Edition* (Eds.: B. L. Feringa, W. R. Browne), Wiley-VCH, **2011**.
- [26] V. Balzani, P. Ceroni, A. Juris, *Photochemistry and Photophysics: Concepts, Research, Applications*, Wiley-VCH, Weinheim, **2014**.
- [27] *Handbook of Photochemistry, Third Edition* (Eds.: M. Montalti, A. Credi, L. Prodi, M. T. Gandolfi), Taylor and Francis, New York, **2006**.
- [28] V. May, O. Kühn, *Charge and Energy Transfer Dynamics in Molecular Systems*, Wiley-VCH, Weinheim, **2000**.
- [29] *Electron Transfer in Chemistry* (Ed.: V. Balzani), Wiley-VCH, Weinheim, **2001**.
- [30] J. R. Lakowicz, *Principles of Fluorescence Spectroscopy, 3rd Ed.* Springer, Singapore, **2006**.
- [31] V. Balzani, F. Bolletta, M. T. Gandolfi, M. Maestri, *Top. Curr. Chem.* **1978**, *75*, 1.
- [32] A. Lavie-Cambot, C. Lincheneau, M. Cantuel, Y. Leydet, N. D. McClenaghan, *Chem. Soc. Rev.* **2010**, *39*, 506, and references therein.
- [33] N. J. Turro, V. Ramamurthy, J. C. Scaiano, *Modern Molecular Photochemistry of Organic Molecules*, University Science Books, Sausalito, **2010**.
- [34] *Photochemistry and Photophysics of Coordination Compounds I and II* (Eds.: V. Balzani, S. Campagna), Springer, Heidelberg, **2007**.
- [35] *Photochromism: Molecules and Systems* (Eds.: H. Dürr, H. Bouas-Laurent), Elsevier, Amsterdam, **2003**.
- [36] M. Baroncini, G. Ragazzon, S. Silvi, M. Venturi, A. Credi, *Pure Appl. Chem.* **2015**, *87*, 537.
- [37] S. Shinkai, T. Nakaji, T. Ogawa, K. Shigematsu, O. Manabe, *J. Am. Chem. Soc.* **1981**, *103*, 111.
- [38] See, e.g.: T. Muraoka, K. Kinbara, T. Aida, *Nature* **2006**, *440*, 512.
- [39] S. Campagna, F. Puntoriero, F. Nastasi, G. Bergamini, V. Balzani, in *Photochemistry and Photophysics of Coordination Compounds I* (Eds.: V. Balzani, S. Campagna), Springer, Heidelberg, **2007**, p. 117.
- [40] B. Colasson, A. Credi, G. Ragazzon, *Coord. Chem. Rev.* **2016**, *325*, 125.
- [41] H. Bouas-Laurent, A. Castellan, J.-P. Desvergne, R. Lapouyade, *Chem. Soc. Rev.* **2001**, *30*, 248.
- [42] P. R. Ogilby, *Chem. Soc. Rev.* **2010**, *39*, 3181.
- [43] S. Cobo, F. Lafalet, E. Saint-Aman, C. Philouze, C. Bucher, S. Silvi, A. Credi, G. Royal, *Chem. Commun.* **2015**, *51*, 13886.
- [44] *Molecular Catenanes, Rotaxanes and Knots. A Journey through the World of Molecular Topology* (Eds.: J.-P. Sauvage, C. Dietrich-Buchecker), Wiley-VCH, Weinheim, **1999**.
- [45] C. Bruns, J. F. Stoddart, *The Nature of the Mechanical Bond: From Molecules to Machines*, Wiley, Hoboken, **2016**.
- [46] A. Tron, H.-P. Jacquot de Rouville, A. Ducrot, J. H. R. Tucker, M. Baroncini, A. Credi, N. D. McClenaghan, *Chem. Commun.* **2015**, *51*, 2810.
- [47] C. Schäfer, G. Ragazzon, B. Colasson, M. La Rosa, S. Silvi, A. Credi, *ChemistryOpen* **2016**, *5*, 120.
- [48] V. Blevé, C. Schäfer, P. Franchi, S. Silvi, E. Mezzina, A. Credi, M. Lucarini, *ChemistryOpen* **2015**, *4*, 18.
- [49] P. R. Ashton, R. Ballardini, V. Balzani, I. Baxter, A. Credi, M. C. T. Fyfe, M. T. Gandolfi, M. Gómez-López, M. V. Martínez-Díaz, A. Piersanti, N. Spencer, J. F. Stoddart, M. Venturi, A. J. P. White, D. J. Williams, *J. Am. Chem. Soc.* **1998**, *120*, 11932.
- [50] A. Arduini, R. Bussolati, A. Credi, S. Monaco, A. Secchi, S. Silvi, M. Venturi, *Chem. Eur. J.* **2012**, *18*, 16203.
- [51] A. Arduini, R. Bussolati, A. Credi, A. Secchi, S. Silvi, M. Semeraro, M. Venturi, *J. Am. Chem. Soc.* **2013**, *135*, 9924.
- [52] G. Ragazzon, M. Baroncini, S. Silvi, M. Venturi, A. Credi, *Beilstein J. Nanotechnol.* **2015**, *6*, 2096.
- [53] M. Baroncini, S. Silvi, M. Venturi, A. Credi, *Chem. Eur. J.* **2010**, *16*, 11580.
- [54] G. Tabacchi, S. Silvi, M. Venturi, A. Credi, E. Fois, *ChemPhysChem* **2016**, *17*, 1913.
- [55] M. Baroncini, S. Silvi, M. Venturi, A. Credi, *Angew. Chem. Int. Ed.* **2012**, *51*, 4223; *Angew. Chem.* **2012**, *124*, 4299.
- [56] G. Ragazzon, M. Baroncini, S. Silvi, M. Venturi, A. Credi, *Nat. Nanotechnol.* **2015**, *10*, 70.
- [57] A. Credi, M. Venturi, V. Balzani, *ChemPhysChem* **2010**, *11*, 3398.
- [58] E. Sevick, *Nat. Nanotechnol.* **2015**, *10*, 18.
- [59] L. Casimiro, J. Groppi, M. Baroncini, M. La Rosa, A. Credi, S. Silvi, *Photochem. Photobiol. Sci.* **2018**, *17*, 734.
- [60] M. Irie, T. Fukaminato, K. Matsuda, S. Kobatake, *Chem. Rev.* **2014**, *114*, 12174.
- [61] P. Naumov, S. Chizhik, M. K. Panda, N. K. Nath, E. Boldyreva, *Chem. Rev.* **2015**, *115*, 12440.
- [62] S. Kobatake, S. Takami, H. Muto, T. Ishikawa, M. Irie, *Nature* **2007**, *446*, 778.
- [63] M. Baroncini, S. d'Agostino, G. Bergamini, P. Ceroni, A. Comotti, P. Sozzani, I. Bassanetti, F. Grepioni, T. M. Hernandez, S. Silvi, M. Venturi, A. Credi, *Nat. Chem.* **2015**, *7*, 634.
- [64] J. R. Holst, A. Trewin, A. I. Cooper, *Nat. Chem.* **2010**, *2*, 915.

- [65] H. Akiyama, M. Yoshida, *Adv. Mater.* **2012**, *24*, 2353.
- [66] H. Yu, *J. Mater. Chem. C* **2014**, *2*, 3047.
- [67] C. Nacci, M. Baroncini, A. Credi, L. Grill, *Angew. Chem. Int. Ed.* **2018**, <https://doi.org/10.1002/anie.201806536>.
- [68] J. M. Pietryga, J.-S. Park, J. Lim, A. F. Fidler, W. K. Bae, S. Brovelli, V. I. Klimov, *Chem. Rev.* **2016**, *116*, 10513, and references therein.
- [69] U. Resch-Genger, M. Grabolle, S. Cavaliere-Jaricot, R. Nitschke, T. Nann, *Nat. Methods* **2008**, *5*, 763.
- [70] *Photoactive Semiconductor Nanocrystal Quantum Dots – Fundamentals and Applications* (Ed.: A. Credi), Springer, Basel, **2016**.
- [71] N. Hildebrandt, C. M. Spillmann, R. W. Algar, T. Pons, M. H. Stewart, E. Oh, K. Susumu, S. A. Diaz, J. B. Delehanty, I. L. Medintz, *Chem. Rev.* **2017**, *117*, 536, and references therein.
- [72] C. J. Bardeen, *Nat. Mater.* **2014**, *13*, 1001.
- [73] M. Amelia, A. Lavie-Cambot, N. D. McClenaghan, A. Credi, *Chem. Commun.* **2011**, *47*, 325.
- [74] S. González-Carrero, M. de la Guardia, R. E. Galian, J. Pérez-Prieto, *ChemistryOpen* **2014**, *3*, 199.
- [75] C. Mongin, S. Garakyaraghi, N. Razgoniaeva, M. Zamkov, F. N. Castellano, *Science* **2016**, *351*, 369.
- [76] M. Tabachnyk, B. Ehrler, S. Gélinas, M. L. Böhm, B. J. Walker, K. P. Musselman, N. C. Greenham, R. H. Friend, A. Rao, *Nat. Mater.* **2014**, *13*, 1033.
- [77] N. J. Thompson, M. W. B. Wilson, D. N. Congreve, P. R. Brown, J. M. Scherer, T. S. Bischof, M. Wu, N. Geva, M. Welborn, T. Van Voorhis, V. Bulović, M. G. Bawendi, M. A. Baldo, *Nat. Mater.* **2014**, *13*, 1039.
- [78] For an example see: G. Ragazzon, P. Verwilt, S. A. Denisov, A. Credi, G. Jonusauskas, N. D. McClenaghan, *Chem. Commun.* **2013**, *49*, 9110.
- [79] M. La Rosa, S. A. Denisov, G. Jonusauskas, N. D. McClenaghan, A. Credi, *Angew. Chem. Int. Ed.* **2018**, *57*, 3104; *Angew. Chem.* **2018**, *130*, 3158.
- [80] Similar results were obtained independently by another research group: C. Mongin, P. Moroz, M. Zamkov, F. N. Castellano, *Nat. Chem.* **2018**, *10*, 225.

---

Received: July 27, 2018